

# Modeling tropospheric wet delays with dense and sparse network configurations for PPP-RTK

P. S. de Oliveira Jr.<sup>1,2,3</sup> · L. Morel<sup>1</sup> · F. Fund<sup>2</sup> · R. Legros<sup>2</sup> · J. F. G. Monico<sup>3</sup> · S. Durand<sup>1</sup> · F. Durand<sup>1</sup>

Received: 21 October 2015 / Accepted: 19 January 2016 / Published online: 2 February 2016  
© Springer-Verlag Berlin Heidelberg 2016

**Abstract** Precise Point Positioning (PPP) is a well-known technique of positioning by Global Navigation Satellite Systems (GNSS) that provides accurate solutions. With the availability of real-time precise orbit and clock products provided by the International GNSS Service (IGS) and by individual analysis centers such as Centre National d'Etudes Spatiales through the IGS Real-Time Project, PPP in real time is achievable. With such orbit and clock products and using dual-frequency receivers, first-order ionospheric effects can be eliminated by the ionospheric-free combination. Concerning the tropospheric delays, the Zenith Hydrostatic Delays can be quite well modeled, although the Zenith Wet

Delays (ZWDs) have to be estimated because they cannot be mitigated by, for instance, observable combinations. However, adding ZWD estimates in PPP processing increases the time to achieve accurate positions. In order to reduce this convergence time, we (1) model the behavior of troposphere over France using ZWD estimates at Orphéon GNSS reference network stations and (2) send the modeling parameters to the GNSS users to be introduced as a priori ZWDs, with an appropriate uncertainty. At the user level, float PPP-RTK is achieved; that is, GNSS data are performed in kinematic mode and ambiguities are kept float. The quality of the modeling is assessed by comparison with tropospheric products published by Institut National de l'Information Géographique et Forestière. Finally, the improvements in terms of required time to achieve 10-cm accuracy for the rover position (simulated float PPP-RTK) are quantified and discussed. Results for 68 % quantiles of absolute errors convergence show that gains for GPS-only positioning with ZWDs derived from the assessed tropospheric modeling are about: 1 % (East), 20 % (North), and 5 % (Up). Since ZWD estimation is correlated with satellite geometry, we also investigated the positioning when processing GPS + GLONASS data, which increases significantly the number of available satellites. The improvements achieved by adding tropospheric corrections in this case are about: 2 % (East), 5 % (North), and 13 % (Up). Finally, a reduction in the number of reference stations by using a sparser network configuration to perform the tropospheric modeling does not degrade the generated tropospheric corrections, and similar performances are achieved.

---

✉ P. S. de Oliveira Jr.  
paulo.de\_oliveira@esgt.cnam.fr

L. Morel  
laurent.morel@esgt.cnam.fr

F. Fund  
francois.fund@geodata-diffusion.fr

R. Legros  
contact@geodata-diffusion.fr

J. F. G. Monico  
galera@fct.unesp.br

S. Durand  
stephane.durand@esgt.cnam.fr

F. Durand  
frederic.durand@esgt.cnam.fr

<sup>1</sup> GeF, Cnam, Le Mans, France

<sup>2</sup> Geodata Diffusion, Paris, France

<sup>3</sup> PPGCC/Unesp, Presidente Prudente, SP, Brazil

**Keywords** GNSS · Float PPP-RTK · ZWD · Tropospheric modeling · Orphéon

## Introduction

The Precise Point Positioning (PPP) technique was first introduced by Zumberge et al. (1997) in the context of processing data from large GPS (Global Positioning System) networks. Following studies proved that this technique is able to provide solutions with an accuracy at the centimeter level (Kouba and Héroux 2001) when using final orbits and clocks solutions produced by the IGS (International Global Navigation Satellite Systems Service). Since then, the number of applications using PPP has grown quickly.

The IGS Real-Time Working Group (IGS-RTWG) established in 2001 investigated the delivery of precise products for real-time PPP applications (Caissy and Agrotis 2011). Gao and Chen (2004) showed that PPP using real-time orbit and clock products can lead to positions with an accuracy at the centimeter level. IGS started the Real-Time Pilot Project in 2007 using GNSS real-time observations from a global network. On April 2013, the IGS Real-time Service (IGS-RTS) was officially launched. However, today official products include only corrections to GPS satellite broadcast orbit and clock products ([www.rtigs.net](http://www.rtigs.net)). The GLONASS corrections are provided as an experimental product and will be included within the service once the RTS reaches its full operating capability. Hadas and Bosy (2015) compared one week of real-time products to European Space Operations Centre (ESOC) final products. Results showed an accuracy of 5 cm for GPS orbits and 8 cm for GPS clocks. The real-time orbit and clock products of individual analysis centers, such as Centre National d'Etudes Spatiales (CNES), have progressively improved (Laurichesse et al. 2009, 2013) and enable promising results for real-time PPP applications with a centimeter accuracy (Ahmed et al. 2014; Shi et al. 2014).

Currently, the quality of real-time satellite orbit and clock products makes the PPP technique a complementary technique to differential GNSS ones like Real-Time Kinematic (RTK) and Network RTK (NRTK). PPP is a State Space Representation (SSR)-based technique which implies that atmospheric effects have to be carefully considered. The first-order ionospheric delay can be mitigated by the ionospheric-free combination for dual-frequency receivers, while tropospheric delays have to be estimated. Tropospheric slant total delays (STDs) are mapped to the receiver's zenith direction using an appropriate mapping function. When processing GNSS data, the resulting Zenith Total Delays (ZTDs) are usually divided in two main components: (1) its hydrostatic part named Zenith Hydrostatic Delay (ZHD) and (2) its non-hydrostatic part, also known as Zenith Wet Delay (ZWD) (Davis et al. 1985).

ZHDs can be easily modeled with good accuracy (Saastamoinen 1972) but not ZWDs as they depend on the water vapor content in the atmosphere, which can vary quickly in time and space. ZWDs are usually estimated as an additional epoch-wise parameter to compute PPP solutions.

The use of external tropospheric information in GNSS processing could reduce high correlations between estimated parameters and so the convergence time of the position. This motivated several studies to generate tropospheric models to produce corrections for positioning applications. These corrections can be generated by means of empirical models, meteorological data, Numerical Weather Prediction (NWP) or directly from modeling the ZTD estimates over a GNSS reference network.

Boehm et al. (2015) introduced the empirical Global Pressure and Temperature 2 wet (GPT2w) model to derive a priori ZWDs from mean values, annual, and semiannual terms for water vapor pressure, weighted average temperature, and the water vapor decay factor. The comparison of this model with the delays estimated by IGS for 341 stations during the year of 2012 presented an average root mean square (RMS) of 3.6 cm.

Ibrahim and EI-Rabbany (2011) analyzed the impacts of using the NWP-based tropospheric corrections of National Oceanic and Atmospheric Administration (NOAA) on ionospheric-free PPP solutions. They concluded that the performance of the model is a function of the season of the year and geographic location. The NWP model improved the PPP solution convergence by 1, 10, and 15 % for the latitude, longitude, and height components, respectively. In recent works at German Research Center for Geosciences (GFZ), Zus et al. (2014) conducted allowing the delivery of real-time tropospheric products as STDs, tropospheric gradients, and mapping functions using NWP models with high speed and precision. Dousa and Elias (2014) described a new concept to derive ZWD using the model of Askne and Nordius (1987) with external meteorological data from numerical weather models. Their approach was superior to existing methods by a factor of 2–3.

Hadas et al. (2013) discussed the impacts of two a priori tropospheric models on simulated float PPP-RTK. The first one was derived from near real-time ZTD estimates on a real-time GNSS network data. The second one was derived from meteorological parameters, such as temperature, pressure, and humidity. The positive impact of tropospheric model application to positioning on convergence time is evidenced but not quantified. Li et al. (2014) presented regional atmospheric augmentation results for the PPP-RTK system in development at the GFZ. Comparable accuracy and convergence time with NRTK were obtained. However, even if the proposed approach uses a sparse network, the solution presented by Li et al. (2014) still

requires a bidirectional link of communication. Shi et al. (2014) introduced a strategy to overcome this limitation with local troposphere corrections. It consists of modeling ZWD estimates inside a real-time GNSS reference network thanks to optimal fitting coefficients (OFCs). This method does not require the a priori knowledge of the user location, since the coefficients can be broadcasted to unlimited number of users. It is quite similar to the low-order surface model also known as partial derivative algorithm presented by Wübbena et al. (1996) and studied by Fotopoulos and Cannon (2001). However, the method described in Shi et al. (2014) can test up to several sets of coefficients by applying different constraints and choosing the optimal set, which makes the method more adaptive.

Concerning PPP in general, the above-mentioned research only indicates that tropospheric corrections can improve its performances, especially the convergence time. However, the use of tropospheric corrections for PPP still needs to be assessed and quantified with a significant amount of data. We focus on methods that need a monodirectional communication link. So, our assessment is dedicated to the use of tropospheric modeling by OFCs in float PPP-RTK. In comparison with Shi et al. (2014), our study is done on a larger area that requires one to go further by using the second-order degree of their mathematical model, what has not been presented before. Also, GNSS data of a real-time reference network well densified over France (160 stations) with a regular distribution (sites interdistances of 60 km) are used and the effect of reducing up to 75 % its density is assessed. In order to consider the weather variability, periods over the four seasons of all year 2014 are selected to be analyzed in the experiments. Finally, we focus on the impact of adding GLONASS data to float PPP-RTK processing.

We describe next the overall strategy employed and the GNSS data used. The assessment and outcomes of the strategies adopted are then discussed, while conclusive considerations are presented in the summary.

## Method, data, and processing

The products and the processing parameters used to estimate the real-time ZWDs at the reference network, as well as the methods employed to obtain ZWDs corrections, are described in this section.

### Methodology

The main inputs as well as the strategy used to accomplish the tropospheric modeling are presented in Fig. 1. In the first step, ZWDs are estimated in real time over a reference GNSS network with station positions strongly constrained

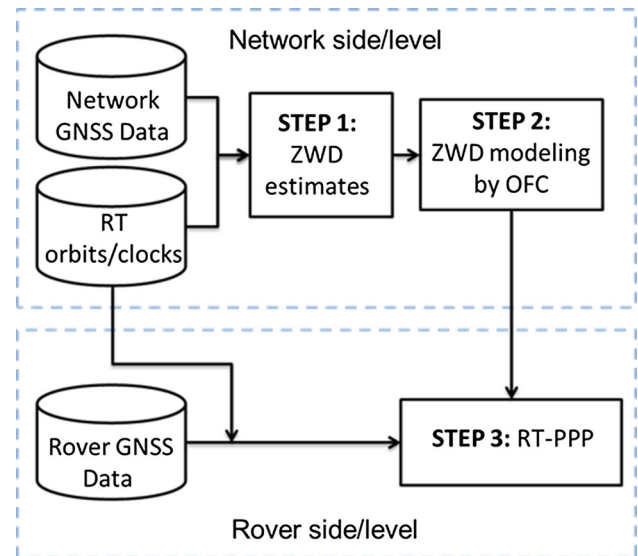


**Fig. 1** Overall strategy to generate and use tropospheric corrections for RT-PPP

(1 cm). In the second step, ZWD estimates are used to generate a model for ZWDs usable at any location in the network area. During this process, quality control parameters are checked to eliminate outliers. Finally, this ZWD model is transmitted to rovers to derive a priori ZWD values used as constraints in the float PPP-RTK algorithm.

In order to perform float PPP-RTK, we use the RTKLib 2.4.2 software (Takasu 2013) modified in this research to have an option to introduce constrained a priori values for the ZWD parameter. Strategies used to estimate ZWDs in the reference GNSS network (step 1) and to perform float PPP-RTK at the rover level (step 3) are summarized in Table 1. The main differences between them are the positioning mode, static or kinematic, and the constrained parameters. During step 1, reference stations coordinates are well known (1 cm), so they are strongly constrained while ZWDs are estimated. At the rover, the receiver coordinates are estimated during step 3, while ZWDs are constrained with a priori ZWD values coming from the tropospheric modeling. Its accuracy is used to constrain tropospheric delays in the PPP-RTK algorithm.

In order to fit conditions of real-time positioning, CNES real-time orbit and clock products are used (Laurichesse et al. 2009). With a cutoff angle of 10 degrees, 30-s sampling GPS and GLONASS measurements are processed. In such conditions, the adoption of a standard tropospheric model for ZHD (Saastamoinen 1972) and the Niell Mapping Functions (NMF) (Niell 1996) does not introduce significant biases with respect to the use of more sophisticated models like GPT2w (Boehm et al. 2015) and GMF (Global Mapping Functions; Boehm et al. 2006) in positioning as verified by Fund et al. (2010).

**Table 1** GNSS processing parameters used at both reference network and rover levels

	GNSS network processing	GNSS rover processing
Mode	PPP static (float solution)	PPP kinematic (float solution)
Orbits and clocks	CNES RT orbit and clock products	CNES RT orbit and clock products
Ionosphere	Ionospheric free	Ionospheric free
Zenith tropospheric delay	ZHD: Saastamoinen (1972) + standard atmosphere ZWD: estimated Mapping functions: Niell (1996)	ZHD: Saastamoinen (1972) + standard atmosphere ZWD: constrained Mapping functions: Niell (1996)
Coordinates	Constrained (1 cm)	Estimated
Elevation mask	10 degrees	10 degrees
Sampling data	30 s	30 s
Kalman process	Forward	Forward
Other parameters	IERS Conventions (2010)	IERS Conventions (2010)
Software	RTKLib 2.4.2 (Takasu 2013)	RTKLib 2.4.2 (Takasu 2013)

### Tropospheric modeling

Once real-time ZWDs at all reference stations are estimated with RTKLib, the OFC for tropospheric modeling are generated. We use a second-order fitting model adapted from Shi et al. (2014),

$$\begin{aligned} \text{ZWD}_i = & a_0 + a_1x_i + a_2y_i + a_3z_i + a_4x_iy_i \\ & + a_5x_iz_i + a_6y_iz_i + a_7x_i^2 + a_8y_i^2 + a_9z_i^2 \\ & (i = 1, \dots, n) \end{aligned} \quad (1)$$

Equation (1) is used with the following constraints (2):

$$0 = \varphi_j a_j \quad (2)$$

with  $\varphi_j = \{0, 1\}$ ,  $j = \{0, \dots, 9\}$

In (1),  $\text{ZWD}_i$  is the ZWD from the reference station  $i$ , and the terms  $(a_0, a_1, \dots, a_9)$  represent the fitting coefficients, which are the parameters to be estimated.  $x_i$ ,  $y_i$ , and  $z_i$  are the geodetic coordinates, and  $j$  is the coefficient number. Different coefficient sets are estimated by increasing the number of constrained coefficients during the least squares adjustment. The number of coefficient sets to be tested ( $c$ ) is given by (3):

$$c = \sum_{k=0}^m \frac{m!}{k!(m-k)!} \quad (3)$$

where  $m$  is the number of coefficients and  $k$  is the number of constrained coefficients ( $a_j$ ). For example, if the number of coefficients is 4 (first-order case),  $c$  is equal to 16. But when the number of coefficients used is 10 (second-order case), the number of coefficient sets tested increases to 1024. The internal quality parameter for the OFC model is the RMS of ZWD residuals at reference stations. The set of OFCs retained is the one that provides the minimal value for the RMS.

### GNSS data

The area studied is France, and GNSS data from two different reference networks in this country are used: (1) the Orphéon GNSS network (Fig. 2) to estimate ZWDs, while (2) the Réseau GNSS Permanent (RGP) is used to assess tropospheric OFCs (Fig. 3, top) and to assess impacts on float PPP-RTK (Fig. 3, bottom).

Periods of the experiment consider the four seasons of the year 2014: 20 days of data distributed over the year (Table 2). Days of each period were chosen taking into account the evolution of daily mean temperatures in France during 2014, published by the official French meteorology agency Météo France (<http://www.meteofrance.fr>) in the climate summary for that year.

#### The Orphéon network

The Orphéon network (<http://reseau-orpheon.fr>) is composed of 160 stations, regularly distributed over France, with baselines of about 60 km long. All the stations have antennas and receivers of the same brand and model (Leica GRX1200 + GNSS or GRX1200GGPRO receivers and Leica AS10 or 1202GG antennas) to guaranty homogeneity of electronic biases. This network is managed by the Geodata Diffusion Company to provide NRTK services in the country.

Two configurations of this network are assessed: (1) a dense network (Fig. 2 top) taking into account the observations from all reference stations and (2) a sparse network (Fig. 2 bottom) composed of only 37 stations, which represents a reduction of about 75 %. Similar relief variation are considered for both network configurations, with a difference of 1651 m between the highest site elevation (1707 m) and the lowest one (56 m).

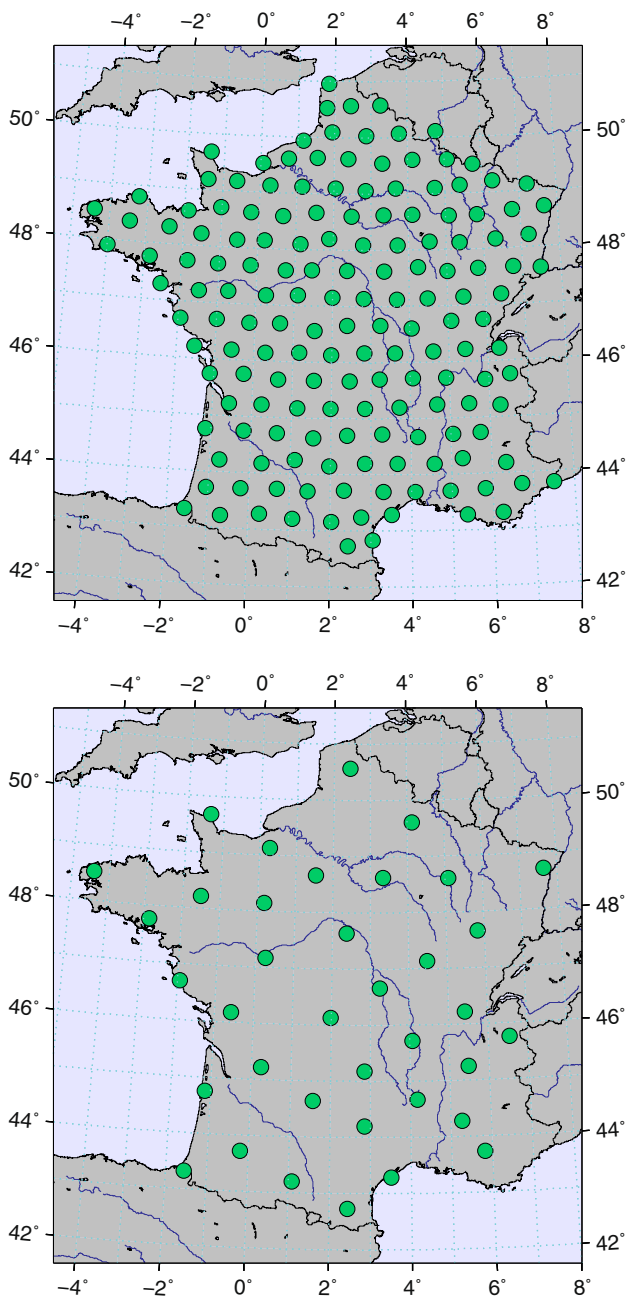


**Fig. 2** The Orphéon GNSS networks used to derive tropospheric OFCs: dense (*top*) and sparse (*bottom*)

### The Réseau GNSS Permanent

The Réseau GNSS Permanent (RGP) is the GNSS network managed by IGN (Institut National de l'Information Géographique et Forestière) which publishes tropospheric ZTDs estimated with the Bernese 5.2 software (Dach and Walser 2015). Figure 3 (*top*) presents all RGP stations that have final ZTD products available at: <ftp://rgpdata.ign.fr/pub/products> during the tested periods. First, these products for all stations, delivered every 15 min, are used as external

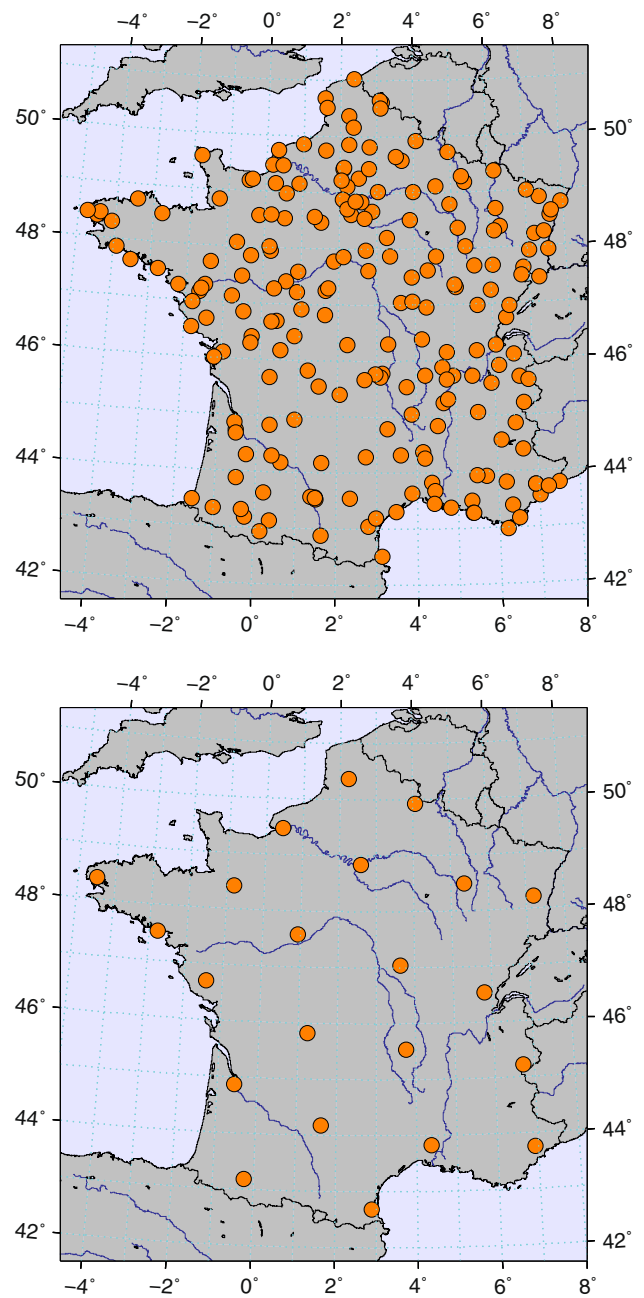


**Fig. 3** The RGP GNSS Networks used to assess tropospheric OFCs derived from Orphéon networks (*top*) and to assess rover positioning (*bottom*)

**Table 2** Periods studied

	Spring	Summer	Autumn	Winter
Days of 2014	121–126	205–210	289–294	357–362

reference to assess the quality of tropospheric OFCs derived from the Orphéon network. Second, only 22 RGP stations regularly distributed over the French territory are used to perform float PPP-RTK at the rover level (Fig. 3

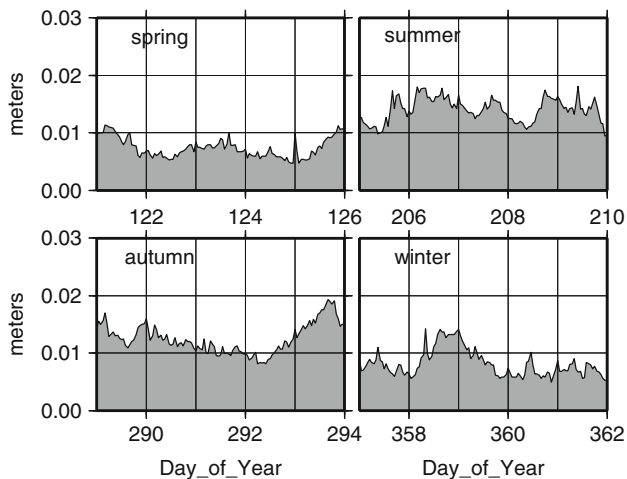


**Fig. 4** RMS of OFC estimates using a dense network

bottom). This network takes into account as much as possible the geographic conditions in France. These stations were chosen considering the quality of their observations in order to avoid multipath effects and noisy measurements.

## Results and analysis

This section presents the results and analysis performed to assess the quality of tropospheric corrections and its impacts on positioning. As stated previously, all results presented here consider simulated real-time positioning conditions.

### Internal quality control

The OFC modeling is performed every hour during the 20 days presented in Table 2. It uses a server model Quad-Core AMD Opteron(tm), Processor 8380 with 2.2 GHz and 40 GB RAM (random access memory). In such conditions, the computer time to test the 1024 coefficient sets and choose the optimal fitting coefficient set is less than 2 or 3 s. The RMS of residuals calculated with the dense and sparse network configurations are presented in Figs. 4 and 5, respectively.

In Fig. 4, we observe that RMS reaches values between 0.6 and 1.8 cm. The highest values appear in summer and autumn. With the sparse network (Fig. 5), values are between 0.6 and 2 cm, so that RMS residuals are quite similar for both network configurations. However, a slightly degradation (about 2 mm) is observed with the dense network.

### External validation

As independent external reference, the 15-min IGN ZTD products estimated using a cutoff angle of 10 degrees are

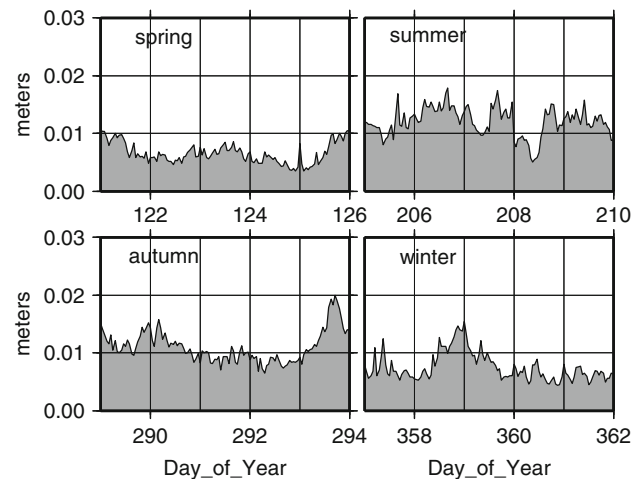


**Fig. 5** RMS of OFC estimates using a sparse network

used to assess tropospheric OFCs. For consistency, ZHDs are computed and subtracted from IGN ZTDs using the parameters described in Table 1.

All stations with ZTD products available (172 stations) are used. A typical IGN ZWD product is shown in Fig. 6 (right). The middle and left panels present tropospheric OFCs derived from dense and sparse reference networks calculated at IGN station locations, respectively.

ZWDs coming from IGN products present values of about 22 cm in the southwestern France, except for a station which is the highest site in France (in the Pyrenees mountain) and consequently located in a drier environment implying ZWD of about 12–14 cm. Since the OFC modeling takes into account height variations, it is possible to reconstruct ZWD values for this station with quite good accuracy. In the northern France, ZWDs are also less significant, about 12–16 cm. This is quite expected considering the latitudinal and relief variations of the French territory. ZWDs modeled from OFCs using dense or sparse reference network configurations present a similar tropospheric surface, but quite less detailed.

The corresponding ZWD differences between IGN products and those from OFCs at IGN station locations are presented in Fig. 7. This example in Fig. 7 shows that the ZWDs derived from OFCs are consistent with IGN products. It means that three solutions plotted in Fig. 6 present similar spatial distributions. Results using the dense configuration present a maximum difference of 4 cm versus  $-3.7$  cm with those using the sparse network. For this example, the hourly mean and standard deviation differences calculated over the whole network are  $0.4 \pm 1.3$  and  $-0.5 \pm 1.4$  cm for the dense and sparse network configurations, respectively.

For all the periods assessed, time series of mean differences over the whole network are presented in Figs. 8

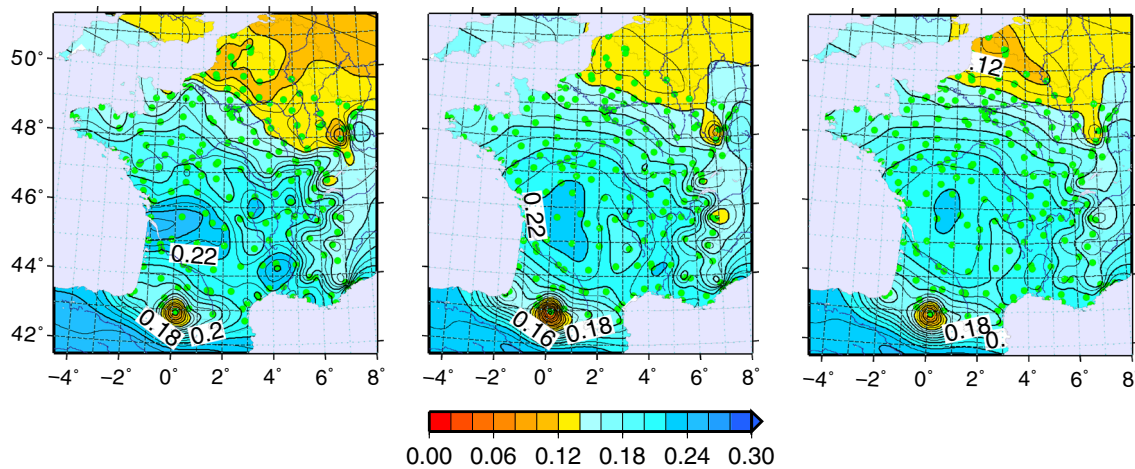


**Fig. 6** Examples of tropospheric ZWD (m) surfaces (day 289/2014—15–16 h): obtained with IGN ZWD products (*right*), OFCs modeling coefficient generated from Orphéon dense (*middle*) and sparse (*left*) network configurations

and 9 for dense and sparse network corrections, respectively. The corresponding standard deviations for these results are presented in Figs. 10 and 11.

Unfortunately, IGN products were not available for day 124. The mean differences with respect to IGN ZWDs for all days assessed in 2014 present a mean bias of  $-4.0$  mm for both network configurations. However, mean differences can reach values up to 4 cm.

In Figs. 10 and 11, the mean STD for all assessed days is 1.2 cm for both dense and sparse network configurations. Worst results are obtained in summer and autumn, especially for the sparse network. It can be due to higher spatial tropospheric gradients that OFCs cannot fit as well as in winter. On the other hand, it shows a good coherence between internal (Figs. 4, 5) and external RMS, which means that the internal quality control is realistic and the residuals RMS is an appropriate parameter to be used as a quality indicator of OFC estimates as well as a constraint for the ZWD at the rover side.

### Impact of tropospheric OFCs on float PPP-RTK

In order to quantify the impacts of using OFCs on positioning, data of IGN stations plotted in Fig. 3 (bottom) are processed in float PPP-RTK over the 20 days of 2014. Processing is re-initialized (cold start) six times per day to assess the impact on convergence time. A time window of 4 h is chosen in order to ensure enough time for convergence to 10-cm accuracy in almost all the cases. Considering the entire experiment over all IGN stations, it gives 2640 cold starts (22 stations  $\times$  20 days  $\times$  6 initializations).

The statistics of positioning errors with respect to the position in ITRF2008 analyzed are median and 68 % quantiles. These statistical parameters are chosen instead of mean and standard deviation due to possible remaining

biases that might cause results that do not follow a Gaussian distribution. Figure 12 presents results (absolute position errors) performed using GPS CNES orbit and clock products on East, North, and Up components, respectively. The blue curve represents the results of standard kinematic PPP with ZWD estimation. About the use of OFCs as a priori ZWDs, two possibilities are also plotted in Fig. 12: (1) OFCs derived from the dense network (violet) and (2) OFCs derived from the sparse network (black). Finally, as a reference solution the float PPP-RTK results with constrained ZWDs provided by IGN over the RGP network (green) are plotted too. The times required for medians and 68 % quantiles to reach 10-cm accuracy is emphasized by vertical bars. We consider the solution has converged at this time.

The results presented in Fig. 12 indicate that OFCs can reduce the convergence time up to 15 min between standard kinematic PPP and PPP-RTK using accurate a priori ZWDs, especially for the Up component. However, the gain on the Up component is more important for median errors while the gain on the North component is more important for 68 % quantile errors. The East component presents the slowest convergence, especially because ambiguities are kept float. Introducing OFCs has only a small impact on convergence time for that component. Detailed results are listed in Table 3.

Concerning median results, using IGN ZWD products performs the shortest time convergence for the Up component: 29.5 min. This represents a gain of 15.5 min (34.4 %) against the standard kinematic PPP (convergence time of 45 min). On that component, positioning using OFC derived from dense and sparse Orphéon configurations shows similar performances. The gains with respect to standard kinematic PPP are 11.5 min (25.6 %; with dense network) and 13 min (28.9 %; with sparse network).

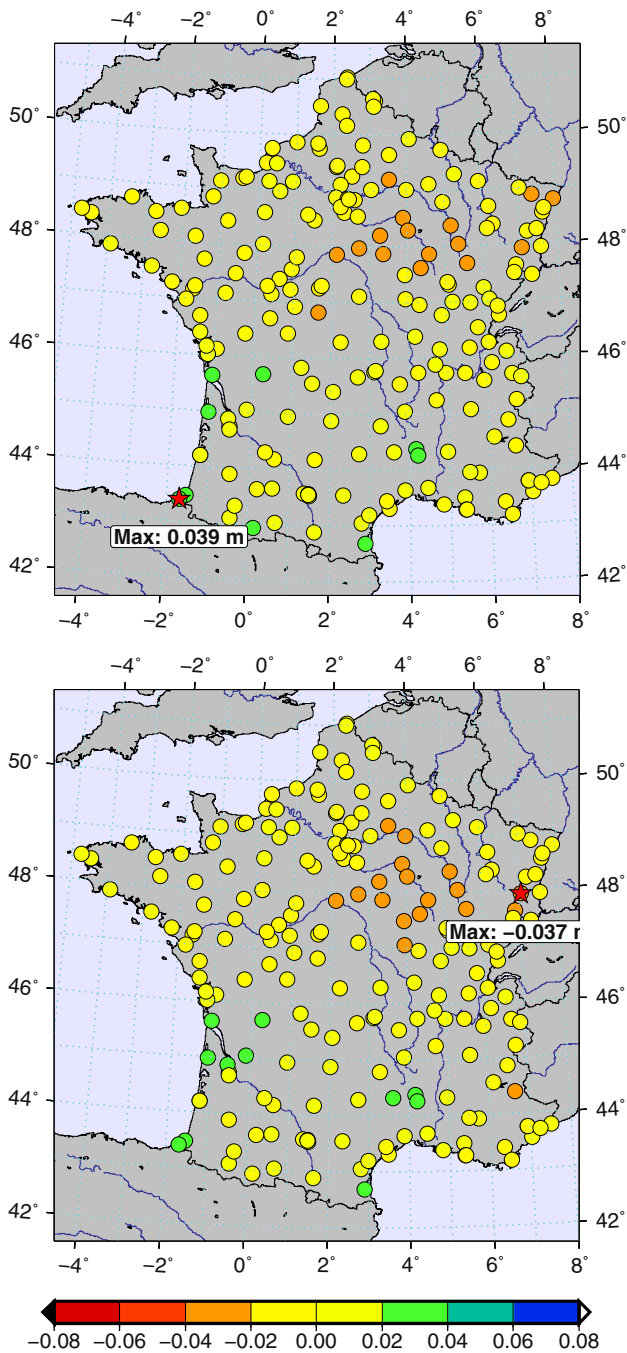


**Fig. 7** Differences (m) between ZWDs provided by IGN and OFCs calculated at RGP site locations using a dense network (*top*) and OFCs calculated at RGP site locations using a sparse network (*bottom*) for the day 289/2014 between 15 and 16 h

The East presents gains of 4.5 min (7.3 %) using IGN ZWDs products, 3.5 min (5.7 %) using OFCs derived from dense network, and 4.5 min (7.3 %) using OFCs derived from sparse network. In North component, these gains are equivalent to 4.0 min (17.8 %) using IGN ZWDs products and 3.5 min (15.6 %) with OFC modeling obtained from dense or sparse network.

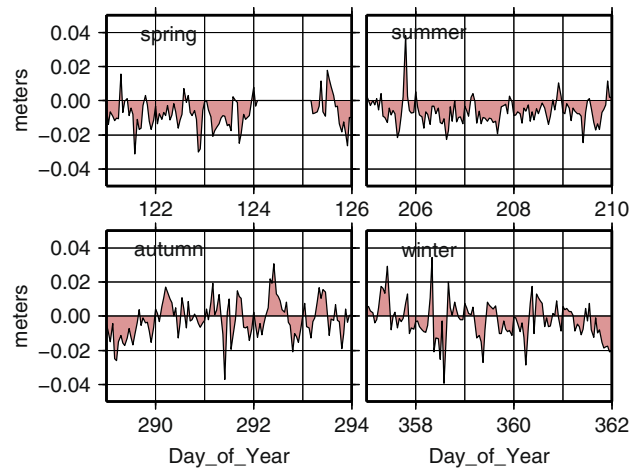


**Fig. 8** Means of the differences between ZWDs provided by IGN and OFCs using a dense network

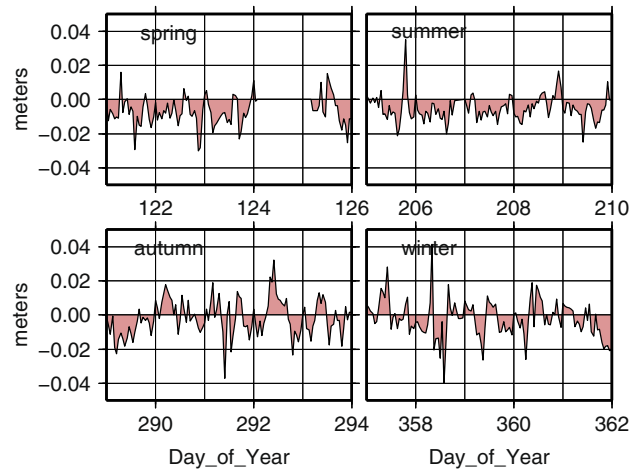


**Fig. 9** Means of the differences between ZWDs provided by IGN and OFCs using a sparse network

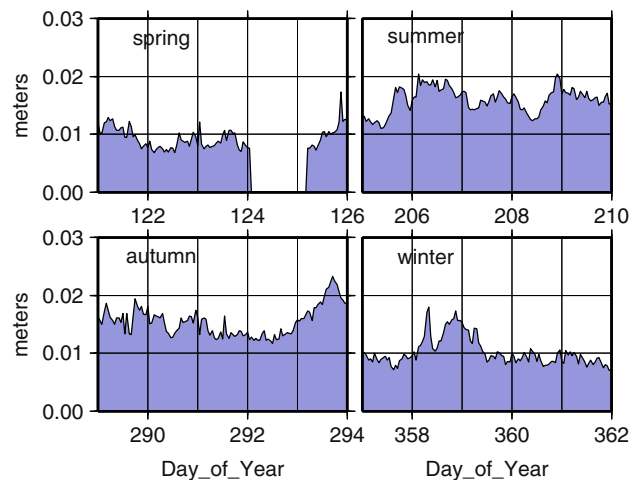


**Fig. 10** STD of the differences between ZWDs provided by IGN and OFCs using a dense network



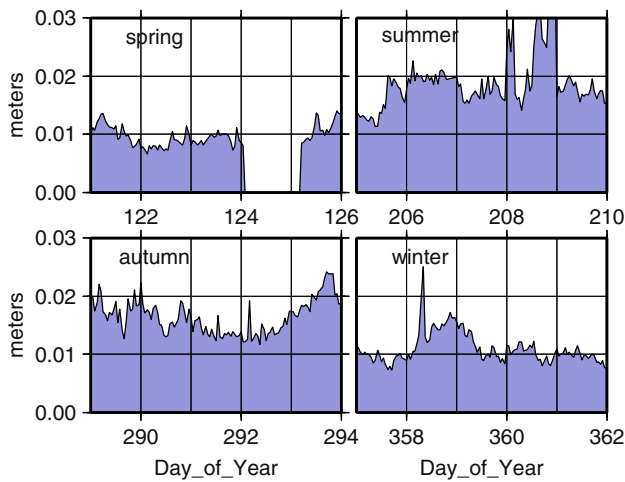


**Fig. 11** STD of the differences between ZWDs provided by IGN and OFCs using a sparse network

**Table 3** Convergence times (min) of PPP-RTK positioning errors (GPS only)

Tropospheric correction	Median Convergence time			68 % quantiles Convergence time		
	E	N	U	E	N	U
Standard (no correction)	61.5	22.5	45.0	95.5	43.5	74.0
IGN ZWD products	57.0	18.5	29.5	92.5	33.0	67.5
OFCs from dense network	58.0	19.0	33.5	94.5	35.0	70.5
OFCs from sparse network	57.0	19.0	32.0	94.5	34.0	69.5

About 68 % quantile results for the Up component, the positioning converged around 74 min. The use of IGN ZWD products decreases the convergence time by 6.5 min, which represents an improvement of 8.8 %. When OFCs derived from dense and sparse networks are used,

- Standard real-time PPP
- float PPP-RTK using IGN 15min product
- float PPP-RTK using Orpheon dense network
- float PPP-RTK using Orpheon sparse network

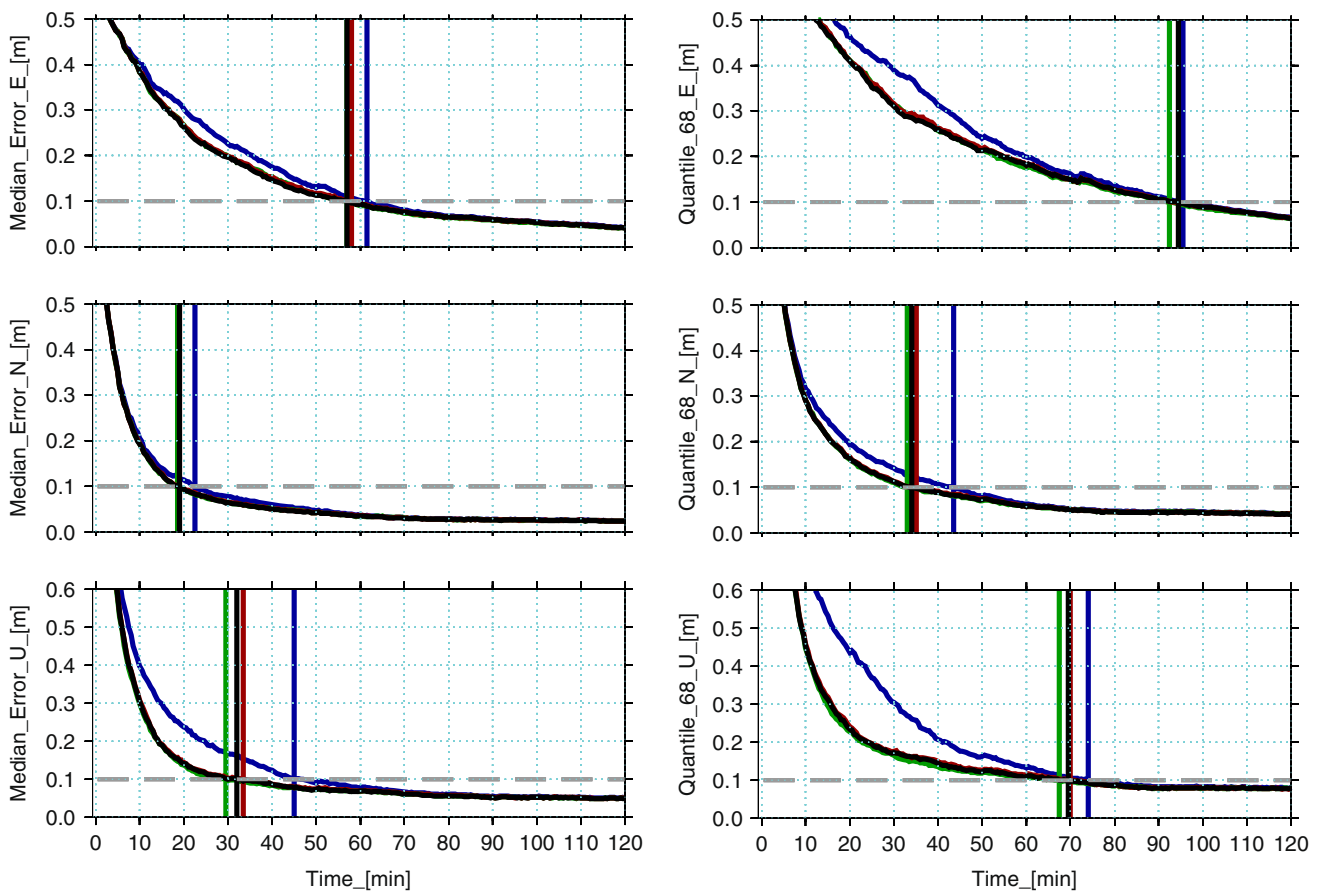


**Fig. 12** Medians (left) and 68 % quantiles (right) of kinematic RT-PPP positioning errors (GPS only) per epoch at IGN stations plotted on Fig. 3 (top)

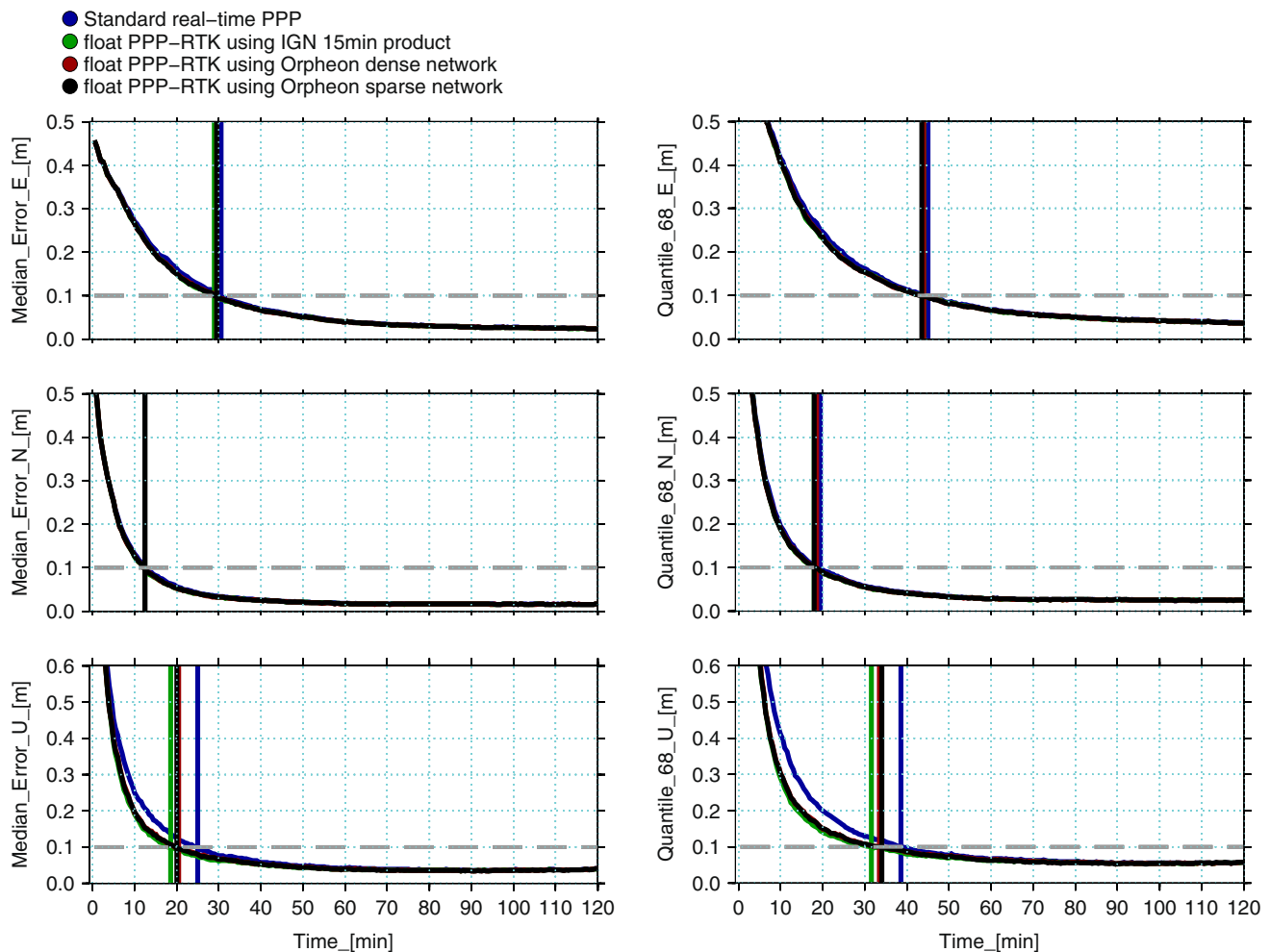


**Fig. 13** Medians (left) and 68 % quantiles (right) of kinematic RT-PPP positioning errors (GPS + GLONASS) per epoch at IGN stations plotted on Fig. 3 (top)

improvements are 3.5 min (4.7 %) and 4.5 min (6.1 %), respectively. The gain in convergence time on the North component with respect to standard kinematic PPP is 10.5 min (24.1 %) when using IGN ZWD products, 8.5 min (19.5 %) when using OFCs derived from dense network, and 9.5 min (21.8 %) when using OFCs derived from sparse network. For the East component, gains are less important since the convergence is much slower than the other components. Indeed, standard kinematic PPP achieved the convergence in 95.5 min and using IGN ZWDs products has an impact of only 3 min (3.1 %). Using OFCs derived from dense and sparse network has no significant impact 1 min (about 1 %).

Using OFCs as a priori ZWDs with GPS + GLONASS observations is also evaluated. Medians and 68 % quantiles of positioning errors are presented in Fig. 13. Detailed results are listed in Table 4. When observations from GLONASS constellation are added to the processing, there is a significant reduction in convergence time with respect

to results obtained with GPS-only processing. It shows that the estimation of tropospheric ZWDs (standard kinematic PPP) is less problematic when the positioning geometry is augmented. More satellites help to decorrelate ZWD and height estimates.

For GPS + GLONASS processing, the median gains observed in convergence time using IGN ZWD products are around 1.5 min (4.9 %) and 6.5 min (26.0 %) on East and Up components, respectively. When applying ZWDs from OFC modeling using dense or sparse network configurations, the same improvements are found on the East component: 1 min (3.3 %). On the height, using OFCs derived from sparse network performed slightly better results with a gain of 5.0 min (20.0 %) against 4.5 min (18.0 %) when using OFCs from dense network configuration. No gain on North component is found with any of the assessed tropospheric corrections.

Results in terms of 68 % quantiles are quite different. Using ZWDs derived from IGN products performs gains of

**Table 4** Convergence times (min) of PPP-RTK positioning errors (GPS + GLONASS)

Tropospheric correction	Median			68 % quantiles		
	Convergence time			Convergence time		
	E	N	U	E	N	U
Standard (no correction)	30.5	12.5	25.0	45.0	19.5	38.5
IGN ZWD products	29.0	12.5	18.5	44.0	18.0	31.5
OFCs from dense network	29.5	12.5	20.5	44.0	18.5	33.5
OFCs from sparse network	29.5	12.5	20.0	43.5	18.0	34.0

1 min (2.2 %) on East, 1.5 min (7.7 %) on North, and 7 min (18.2 %) on Up. Again, the gains achieved using OFC derived from both dense or sparse networks are similar. Indeed, the use of a dense network provides gains of 1.0 min (2.2 %) on East, 1.0 min (5.1 %) on North, and 5.0 min (13.0 %) on Up component, while using a sparse network improves by 1.5 min (3.3 %) on East, 1.5 min (7.7 %) on North, and 4.5 min (11.7 %) on Up. These improvements in 68 % quantiles are comparable to those presented by Ibrahim and El-Rabbany (2011) on ionospheric-free-based PPP with tropospheric corrections derived from NWP modeling in North America. Besides, the relative gains when applying tropospheric corrections in GPS + GLONASS processing are quite comparable with those found in GPS-only results, especially for median.

In order to assess the impact of tropospheric corrections over 2014, Table 5 presents 68 % quantiles of positioning errors over the four periods assessed (spring, summer, autumn, and winter). The most significant achievements with tropospheric corrections are observed in summer, but the convergence time is also the largest among the four periods of the experiment. For GPS-only results using IGN ZWD products, convergence times are improved by 3 min (2.4 %; East), 20 min (42.5 %; North), and 19.5 min (14.0 %; Up). When adding GLONASS data, these improvements become 6 min (9.3 %; East), 2.5 min (12.8 %; North), and 8.5 min (21.5 %; Up). Gains of horizontal components using OFC modeling are quite similar to those using IGN products. However, it is not the case for the Up component whose convergence time is enhanced, up to 13.5 min (34.2 %) and 12.5 min (31.6 %), with dense and sparse network configurations.

During spring and for GPS-only results, the gains achieved with IGN ZWD products are about 2.5 min (3 %; East), 5.0 min (15 %; North), and 9.5 min (19 %; Up). When GPS + GLONASS positioning is performed these gains are 2.0 min (6 %; East), 0.5 min (2 %; North), and 12 min (32 %; Up). The use of OFC modeling presents very close performances for this period, using GPS only or GPS + GLONASS, except for the Up component of

GPS + GLONASS results where the improvement is 22.7 % with both network configurations.

During autumn the gains achieved with IGN ZWD products are 5.5 min (7.6 %; East), 8 min (15.5 %; North), and 8 min (11 %; Up) for only GPS results. Performances using the OFC modeling are about 4 min (6 %; East), 5 min (10 %; North), and 4 min (6 %; Up). For GPS + GLONASS results, only small improvements are verified even if some small negative impacts are observed for the Up component.

During winter the tropospheric corrections improve only the convergence of the Up component with GPS and GPS + GLONASS. On the other hand, the horizontal convergence time is even slightly degraded.

## Summary

Since PPP is a SSR-based technique, the atmospheric effects have to be considered carefully. One of these effects is the tropospheric ZTD, which has a residual component (ZWD) that must be estimated as an additional parameter in GNSS processing. However, the use of accurate a priori ZWDs helps to reduce the convergence time of the position.

In order to reduce the time required for PPP-RTK to converge to 10-cm accuracy, this work has focused on two points: (1) tropospheric modeling to provide network-based ZWD corrections and (2) the impacts of using such a model to constrain a priori ZWDs in PPP-RTK processing. The OFC modeling technique (Shi et al. 2014) is used because it requires only a monodirectional communication link. Improvements of constraining a priori ZWDs on convergence time have been assessed with dense and sparse networks as well as with GPS only and with GPS + GLONASS data. Twenty days distributed in four main periods along the year 2014 are selected. These periods were chosen according to the seasons of the year and the annual temperature variations in France as published by Météo-France.

As an independent external reference, the IGN ZTD products are used to assess tropospheric ZWD modeled by OFCs. The modeled ZWDs present an accuracy of around 1.3 cm with respect to IGN ZTDs. In addition, a good consistency between the RMS of residuals and the differences with respect to the IGN products is found.

Improvements of convergence time when using tropospheric corrections for PPP-RTK are quantified. In terms of 68 % quantiles, gains on convergence time are 1 % on East, about 20 % on North, and about 5 % on Up when using GPS only. Introducing GLONASS data shortens by about 50 % the convergence time of all components. However, adding tropospheric corrections when processing

**Table 5** 68 % quantile of convergence times (min) over 2014

Tropospheric corrections	GPS only Convergence time to 10 cm accuracy			GPS + GLONASS Convergence time to 10 cm accuracy		
	E	N	U	E	N	U
<i>Spring</i>						
Standard (no correction)	84.5	34.0	49.5	33.0	20.5	37.5
IGN ZWD products	82.0	29.0	40.0	31.0	20.0	25.5
OFCs from dense network	83.0	29.0	40.0	31.5	19.5	29.0
OFCs from sparse network	82.0	30.0	40.5	31.5	19.5	29.0
<i>Summer</i>						
Standard (no correction)	124.5	47.0	139.5	64.5	19.5	39.5
IGN ZWD products	121.5	27.0	120.0	58.5	17.0	31.0
OFCs from dense network	121.5	29.0	120.0	64.5	17.0	26.0
OFCs from sparse network	121.5	29.5	123.0	58.5	17.0	27.0
<i>Autumn</i>						
Standard (no correction)	72.5	51.5	72.5	45.0	18.5	38.0
IGN ZWD products	67.0	43.5	64.5	44.0	18.0	38.0
OFCs from dense network	68.5	47.0	69.5	44.0	18.5	39.0
OFCs from sparse network	68.0	45.0	67.0	44.0	18.0	39.0
<i>Winter</i>						
Standard (no correction)	104.5	26.5	61.5	46.5	17.5	41.0
IGN ZWD products	104.5	31.0	45.0	46.5	17.0	33.0
OFCs from dense network	106.0	31.0	47.5	46.5	18.0	36.0
OFCs from sparse network	106.0	31.0	48.0	46.5	18.0	38.5

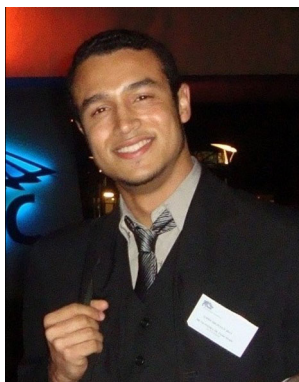
GPS + GLONASS data only improves horizontal positioning by about 2 % on East and about 6 % North, but height is improved by about 12 % Up. In summer and autumn due to more relevant tropospheric activity, the positions convergence takes more time. Even if ZWD modeling does not fit tropospheric delays as well as in winter, using a priori ZWDs derived from dense or sparse networks improves the convergence time. Finally, a reduction in the number of reference stations by using a sparser network configuration does not degrade the generated tropospheric corrections derived from OFCs, and similar performances are achieved between the two configurations.

**Acknowledgments** This project is funded by the French company Geodata Diffusion together with the Brazilian National Council of Technological and Scientific Development (CNPq; *Conselho Nacional de Desenvolvimento Científico e Tecnológico*) and the French National Research Agency (ANRT; *Association Nationale de la Recherche et de la Technologie*). The authors thank the reviewers for their attention and valuable contributions during the review of this paper.

## References

- Ahmed F, Václavovic P, Teferle FN, Dousa J, Bingley R, Laurichesse D (2014) Comparative analysis of real-time precise point positioning zenith total delay estimates. *GPS Solut*. doi:[10.1007/s10291-014-0427-z](https://doi.org/10.1007/s10291-014-0427-z)
- Askne J, Nordius H (1987) Estimation of tropospheric delay for microwaves from surface weather data. *Radio Sci* 22(3):379–386
- Boehm J, Niell A, Tregoning P, Schuh H (2006) Global Mapping Function (GMF): a new empirical mapping function based on numerical weather model data. *Geophys Res Lett* 33:L07304
- Boehm J, Möller G, Schindelegger P, Pain G, Weber R (2015) Development of an improved blind model for slant delays in the troposphere (GPT2w). *GPS Solut*. doi:[10.1007/s10291-014-0403-7](https://doi.org/10.1007/s10291-014-0403-7)
- Caissy M, Agrotis L (2011) Real-time working group and real-time pilot project. *Int GNSS Serv Tech Rep* 2011:183–190
- Dach R, Walser P (2015) Bernese GNSS Software Version 5.2: tutorial processing example—introductory course, terminal session. Astronomical Institute, University of Bern
- Davis JL, Herring TA, Shapiro II, Rogers AEE, Elgered G (1985) Geodesy by radio interferometry: effects of atmospheric modeling errors on estimates of baseline length. *Radio Sci* 20:1593–1607
- Dousa J, Elias M (2014) An improved model for calculating tropospheric wet delay. *Geophys Res Lett* 41:4389–4397. doi:[10.1002/2014GL060271](https://doi.org/10.1002/2014GL060271)
- Fotopoulos G, Cannon ME (2001) An overview of multi-reference station methods for cm-level positioning. *GPS Solut* 4(3):1–10
- Fund F, Morel L, Mocquet A, Boehm J (2010) Assessment of ECMWF derived tropospheric delay models within the EUREF Permanent Network. *GPS Solut* 39–48. doi:[10.1007/s10291-010-0166-8](https://doi.org/10.1007/s10291-010-0166-8)
- Gao Y, Chen K (2004) Performance analysis of precise point positioning using real-time orbit and clock products. *J GPS* 3(1–2):95–100

- Hadas T, Boky J (2015) IGS RTS precise orbits and clocks verification and quality degradation over time. *GPS Solutions* 19:93–105. doi:10.1007/s10291-014-0369-5
- Hadas T, Kaplon J, Boky J, Sierny J, Wilgan K (2013) Near-real-time regional troposphere models for the GNSS precise point positioning technique. *Meas Sci Technol* 24:055003
- Ibrahim H, El-Rabbany A (2011) Performance analysis of NOAA tropospheric signal delay model. *Meas Sci Technol* 22:115107
- IERS Conventions (2010) Gérard Petit and Brian Luzum (eds). (IERS Technical Note; 36) Frankfurt am Main: Verlag des Bundesamts für Kartographie und Geodäsie, 2010, 179 pp, ISBN 3-89888-989-6
- Kouba J, Héroux P (2001) GPS precise point positioning using IGS orbit products. *GPS Solut* 5(2):12–28
- Laurichesse D, Mercier F, Berthias JP, Broca P, Cerri L (2009) Integer ambiguity resolution on undifferenced GPS phase measurements and its application to PPP and satellite precise orbit determination. *Navig J Inst Navig* 56(2):135–149
- Laurichesse D, Cerri L, Berthias JP, Mercier F (2013) Real time precise GPS constellation and clocks estimation by means of a Kalman filter. In: Proceedings of ION GNSS-13, Institute of Navigation, Nashville, Tennessee, pp 1155–1163
- Li X, Dick G, Ge M, Heise S, Wickert J, Bender M (2014) Real-time GPS sensing of atmospheric water vapor: precise point positioning with orbit, clock, and phase delay corrections. *Geophys Res Lett* 41. doi:10.1002/2013GL058721
- Niell A (1996) Global mapping functions for the atmosphere delay at radio wavelengths. *J Geophys Res* 101:3227–3246
- Saastamoinen J (1972) Atmospheric correction for the troposphere and stratosphere in radio ranging of satellites. The use of artificial satellites for geodesy. *Geophys Monogr* 15(3):247–251
- Shi J, Xu C, Guo J, Gao Y (2014) Local troposphere augmentation for real-time precise point positioning. *Earth Planets Space* 66:30
- Takasu T (2013) RTKLIB ver. 2.4.2: Manual
- Wübbena G, Bagge A, Seeber G, Volker B, Hankemeier P (1996) Reducing distance dependent errors for real-time precise DGPS applications by establishing reference station networks. In: Proceedings of ION GPS-96, Institute of Navigation, Kansas City, Missouri, pp 1845–1852
- Zumberge JF, Hefflin MB, Jefferson DC, Watkins MM, Webb FH (1997) Precise point positioning for the efficient and robust analysis of GPS data from large networks. *J Geophys Res* 102:5005–5017
- Zus F, Dick G, Dousa J, Heise S, Wickert J (2014) The rapid and precise computation of GPS slant total delays and mapping factors utilizing a numerical weather model. *Radio Sci* 49(3):207–216



development of atmospheric modeling for real-time GNSS positioning.

**Paulo Sérgio de Oliveira Jr.** graduated from UNESP (*Sao Paulo State University*) in Geomatics Engineering in 2013. He obtained the M.Sc. degree from the same institution with studies in tropospheric effects modeling and GNSS positioning. Currently, he is a Ph.D. student at CNAM (*Conservatoire National des Arts et Métiers*) under cosupervision at Unesp and a member of the R&D team of Geodata Diffusion company.

His research is focused on the



**Laurent Morel** is an assistant professor at the school of engineering ESGT (Ecole Supérieure des Géomètres Topographes) at Le Mans in France. He is involved in many aspects of positioning and the troposphere since 2005.



positioning in real time.

**François Fund** obtained his Ph.D. in space geodesy applied to tropospheric delays and ocean tide loading in 2009 from the University of Nantes, France. Then, he conducted research about Precise Point Positioning at CNES in Toulouse, France. He is now a system engineer at the Geodata Diffusion company, subsidiary of Hexagon Geosystems. He manages the French GNSS Orpheon network and follows R&D activities about point



positions. Since 2015, he has left Geodata Diffusion and is still creating and developing new businesses in the range of precise GNSS.

**Romain Legros** graduated in 2003 from The French National School of Geographic Sciences (ENSG) which was founded to train technical personnel for the National Institute of Geographic and Forest Information (IGN). In 2004, he installed the first permanent stations of the real-time GNSS network Orphéon. In 2006, he became CEO of the Geodata Diffusion company dedicated to manage this network which today includes more than 160 permanent stations.



**João Francisco Galera Monico** received his B.Sc. degree in Cartographic Engineering in 1982, M.Sc. in Geodetic Science in 1982, and Ph.D. in Space Geodesy in 1995. From 2005 to 2013, he was an Adjunct Professor at the Department of Cartography, UNESP at Presidente Prudente, SP, Brazil, where he was lecturing and researching topics related to GNSS, especially those applied to Geodesy, Surveying, and Atmospheric Sci-

ences. Now, he is a Researcher also with UNESP at the same Department.



**Frédéric Durand** is an engineer at the school of engineering ESGT at Le Mans in France. In recent years, he has been involved with many projects about geodesy and satellite positioning.



**Stéphane Durand** is an assistant professor at the school of engineering ESGT at Le Mans in France. His studies are concentrated in GNSS positioning and estimation processes.